Electrical Stimulation Enhance Neural Regeneration and Locomotor Function in Complete Spinal Cord Injury of Rats

Aihua Wang [1, a], Tongtong Zhao [2, b], Lei Wang [2, c] and Yanyan Chen [2, d]

[1] School of Optical and Electronic Information, Suzhou City University, Suzhou, MA 215104, China;

[2] Suzhou Institute of Nano-Tech and Nano-Bionics, Chines Academy of Sciences, China.

[a] wangah@szcu.edu.cn, [b] ttzhao2020@sinano.ac.cn, [c] lwang2020@ sinano.ac.cn,

[d] yychen2006@ sinano.ac.cn

Abstract. Spinal cord injury (SCI) leads to devastating functional loss, partly due to a hostile post-injury microenvironment characterized by detrimental events like excessive calcium influx and apoptosis, which also limit the efficacy of reparative strategies such as neural tissue transplantation. It has been reported that electrical stimulation (ES) could modulate these events. Here, we investigated whether ES could enhance SCI repair, particularly when combined with allogeneic adult spinal cord tissue (aSCT) transplantation. Adult rats with complete thoracic SCI received aSCT grafts, with a subset also receiving continuous ES for two weeks. It found that locomotor function was significantly improved in rats receiving ES in conjunction with transplantation compared to those with transplantation alone. Histologically, ES treatment markedly enhanced neuronal survival and increased GAP-43$^+$ axonal fiber density in the injured spinal cord. Mechanism studies revealed that ES downregulated L-type voltage-gated calcium channel (L-VGCC) and cleaved Caspase-3 expression. These results indicate that ES, when applied with aSCT transplantation, significantly promotes motor functional recovery and neural repair by mitigating calcium influx and apoptosis. Therefore, ES could be considered as a potent therapeutic strategy to augment reparative processes for SCI.

Keywords: Electrical stimulation; spinal cord injury; neural repair; calcium influx; apoptosis.

1. Introduction

Primary mechanical trauma in spinal cord injury (SCI) rapidly triggers complex secondary injury cascades. It exacerbating tissue destruction and creating a hostile microenvironment that severely impedes neural regeneration and functional recovery [1-3]. Neural tissue transplantation, such as the transplantation of adult spinal cord tissues (aSCTs), aim to treat SCI by bridging the lesion, replacing cells, and providing a reparative scaffold [4, 5]. Compared to cell transplantation, aSCTs possess an inherent extracellular matrix, organized architecture, and all cell types, enabling more direct replacement of damaged tissue. However, due to the hostile post-injury microenvironment, transplanted aSCTs exhibit low survival and poor functional integration within the host. So the therapeutic efficacy was significantly diminishing [6]. A major contributor to this detrimental microenvironment was the excessive calcium influx after SCI [7, 8].

As a therapeutic intervention, electrical stimulation (ES) could promote neuronal survival, guide axonal growth, and modulate inflammatory processes [9-11]. Interestingly, some studies suggested ES can influence ion channel activity and cellular excitability [12], offering a means to counteract early detrimental Ca^{2+} influx post-SCI. Our previous work has correlated ES parameters with injury potentials and demonstrated that specific ES could modulate these injury-related events [13, 14]. Therefore, we hypothesized that ES could create a more favorable microenvironment, thereby enhancing the outcomes of the transplanted aSCTs, by directly mitigating early triggers of secondary injury like calcium overload and apoptosis.

In this study, we investigated the efficacy of ES as a strategy to improve SCI repair, implemented in conjunction with allogeneic aSCT transplantation. The effects of ES were systematically evaluated on functional recovery, neuronal survival, and axonal regeneration. Furthermore, potential underlying mechanisms were elucidated through transcriptome sequencing

analysis and Western blotting (WB). This study aims to determine whether ES can act as an effective local microenvironment modulator to improve prognosis following SCI, particularly by targeting critical early pathological events.

2. Materials and Methods

2.1 Surgery Procedures

Adult female Sprague-Dawley (SD) rats were purchased from Shanghai SLAC Laboratory Animal Co., Ltd. (Shanghai, China). All the rats were randomly assigned into two parts: recipient and donor rats. Animal housing conditions and experimental procedures were approved by the Animal Welfare Committee of the Suzhou Institute of Nano-Tech and Nano-Bionics, Chinese Academy of Sciences.

The procedure for the complete transection of the thoracic spinal cord was similarly to the method described by Fan et al. [15]. Briefly, a longitudinal midline incision was made dorsally to expose the T7-T12 vertebrae. Laminectomies were then performed at the T8, T10, and T12 vertebral levels to expose the underlying spinal cords. The spinal cord at the T10 level was completely transected, and an approximately 4 mm segment was removed. Bleeding at the injured site was controlled by using gelatin sponges. All SCI rats were randomly divided to two groups: control group rats, which received aSCTs transplantation; and ES group rats, which applied ES combined with aSCTs transplantation.

The procedure for allogeneic aSCTs transplantation was performed as described by Shen et al. [4]. To obtain the graft tissues, the T9-T10 spinal cord segment of donor rats was exposed and transected using the same method as described above. The spinal cords were then carefully dissected and immediately placed in ice-cold artificial cerebrospinal fluid. After gently blotting the surface with a gelatin sponge, they were transplanted into the lesion sites in the recipient rats with its normal orientation. Subsequently, 40 μL collagen gel biomaterial was slowly injected into each the graft- host interface by microsyringe. In order to mitigate graft rejection, all recipient rats received daily intraperitoneal injections of Cyclosporin A (10 mg/kg).

For the ES application, the procedure was performed as we previously described [13]. Two identical electrical stimulators were used for each rat. The stimulation electrodes were spiral electrodes (diameter 1 mm) fabricated from 0.2 mm diameter platinum-iridium alloy wire (90% Pt, 10% Ir). Two anodes of the stimulators were sutured at the paravertebral muscles on both sides of the T10 level. Two cathodes were sutured to the paravertebral muscles at the T8 and T12 levels, respectively. The distance between adjacent electrodes was approximately 1 cm. Immediately Post-SCI, the stimulators were switched on, delivering continuous direct current ES (1.1 V) for 2 weeks. After suturing the muscle incision, the main body of the stimulator was secured subcutaneously before the skin wound was closed. Rats in the control group also had stimulation electrodes implanted and sutured in the same configuration as described above, but the stimulator was not switched on.

2.2 Behavioural Assessment

The Basso, Beattie, and Bresnahan (BBB) scale was used to assess the recovery of hindlimb locomotor function in rats. Two investigators who were blinded to the experimental group assignments evaluated the BBB score at the different time points after surgery, and the average score was taken as the final score for each time point. During the assessment period, rats were placed in an open field, and observers evaluated their hindlimb joint movement, limb movement, coordination, and gait to determine the final BBB score.

2.3 Immunofluorescence Staining

At 8 weeks post-surgery, spinal cord from T5-L2 was collected and longitudinal sectioned into 16 μm thickness slides. After antigen retrieval, the sections were incubated with 0.3% Triton X-100

solution, and blocked with 5% BSA in PBS for 2 h at room temperature (RT) to prevent non-specific antibody binding, which were then incubated overnight at 4°C with primary antibodies. Following rinsing using PBS, the sections were incubated with corresponding secondary antibodies for 2 h at RT. Primary antibodies used were anti-GFAP (1:1000, ab4674, Abcam), anti-Tuj-1 (1:200, ab18207, Abcam), anti-MAP2 (1:500, ab11267, Abcam), and anti-GAP-43 (1:1000, 5307, Cell Signaling). Images were captured with an Olympus FV3000 confocal microscope under the same parameters, and the immunofluorescence intensity was quantified by ImageJ software.

2.4 Western Blot

At 1 and 2 weeks post-injury, the rats were sacrificed and the spinal cord centered at the lesion site were harvested, which were lysed in RIPA buffer. After centrifugation (12000 rpm for 10 min), supernatants were collected and denatured in 1x SDS loading buffer for 10 min at 98°C. Protein samples were then separated in SDS–PAGE gel and transferred to PVDF membranes (Millipore). Following blocking in 5% non-fat milk for 1 h at RT, the membranes were incubated with primary antibodies overnight at 4°C, and HRP-conjugated secondary antibodies for 2 h at RT. The primary antibodies used were anti-GAPDH (1:5000, 60004-1-Ig, proteintech), anti-L-VGCC (1:200, sc-398995, Santa Cruz Biotechnology), and anti-cleaved-caspase-3 (1:1000, 9661, Cell Signaling).

2.5 RNA-sequencing Analysis

At 2 weeks after surgery, the spinal cords at the injury sites were isolated, and total RNA was extracted using Trizol reagent (Invitrogen) for RNA-seq analysis (OE Biotech Co., Ltd., Shanghai, China). In order to unravel the function of genes regulated by the ES, Gene ontology (GO) and Kyoto Encyclopedia of Genes and Genomes (KEGG) analysis were performed.

2.6 Statistical Analysis

Statistical analysis and graph drawing were performed by GraphPad Prism. All data were presented as mean ± standard deviation. The significant differences between groups were assessed using one-way ANOVA followed by Tukey's post hoc test. $P < 0.05$ was considered significant.

3. Results and Disscussion

3.1 Restoration of Locomotor Function

Regenerative effect of ES on SCI repair was evaluated by assessing locomotor function in rats. Fig. 1 shows the time course of BBB score recovery over 8 weeks post-injury for both control and ES groups. Prior to spinal cord transection, all rats exhibited a BBB score of 21, which dropped to 0 post-injury, indicating a complete loss of hindlimb locomotor function. The BBB scores of the control group rats gradually increased, reaching 5.43 ± 1.62 at 8 weeks post-surgery. It suggested that allogeneic aSCTs transplantation alone could restore some motor function after SCI, which was consistent with the results reported by Shen et al. [4]. By contrast, the ES group rats showed higher BBB scores, and a significant difference was not observed until 4 weeks post-surgery. It suggested that ES promoted the recovery of motor function when combined with aSCT transplantation.

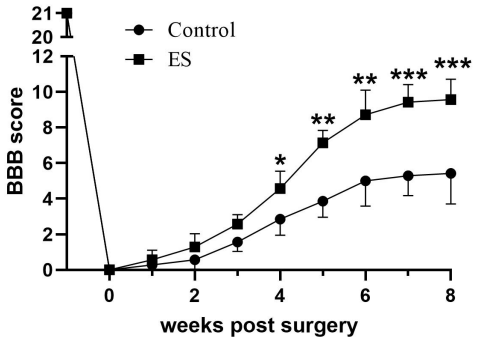

Fig. 1 The score change of BBB over time. Compared to the control, ES group exhibited significant higher BBB scores from week 4 to week 8 post-surgery. *$P < 0.05$, **$P < 0.01$, ***$P < 0.001$.

3.2 Promotion of Neuronal Survival

To evaluate the survival of transplanted allogeneic aSCTs within the host microenvironment following the ES application, Tuj-1 and MAP-2 immunofluorescence staining was performed at 8 weeks post-surgery. Only a few Tuj-1 positive cells were observed within the spinal cord in the control group at the lesion site. By contrast, a large number of Tuj-1 positive cells were observed in the ES group (Fig. 2A). The level of Tuj-1 staining around either the lesion zone or the lesion's edge in the ES group were significantly higher than that in the control group (Fig. 2C, D). The expression pattern of MAP-2 was similar to that of Tuj-1. At 8 weeks post-surgery, the expression level of MAP-2 in the ES group was significantly higher than in the control group, both in the lesion zone and at the lesion edge (Fig. 2B, E, and F).

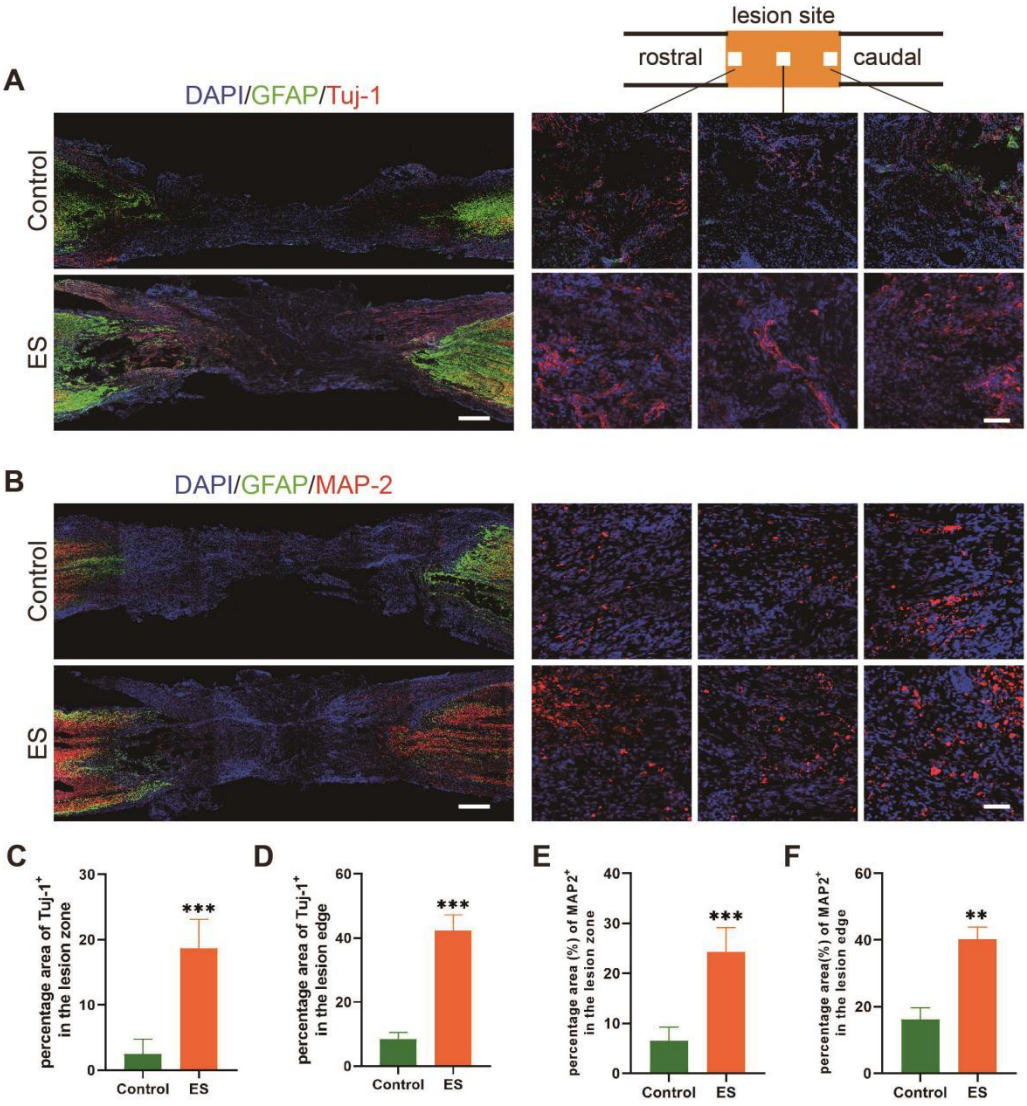

Fig. 2 Neuronal survival at the SCI site. (A) Representative images of Tuj-1 immunostaining in different groups at 8 weeks post-surgery. (B) Representative images of MAP-2 immunostaining in different groups at week 8. (C) Percentage of Tuj-1$^+$ area in the lesion zone. (D) Percentage of Tuj1$^+$ area in the lesion edge. (E) Percentage of MAP-2$^+$ area in the lesion zone. (F) Percentage of MAP-2$^+$ area in the lesion edge. In the left and right images of (A) and (B), the scale bars represent 500 μm and 50 μm, respectively. $^{**}P < 0.01$, $^{***}P < 0.001$.

After complete SCI, there is extensive loss of tissue and cells at the lesion site. Cell and tissue transplantation can replace these lost neural cells and tissues, thereby exerting a therapeutic effect on SCI [16]. However, due to the inhibitory microenvironment, the survival rate of transplanted cells and tissues is often low, which greatly diminishes the therapeutic efficacy of such transplantation strategies. Immunofluorescence staining results demonstrate that ES application combined with allogeneic aSCTs transplantation significantly increased the number of surviving neurons, which confirmed by Tuj-1 and MAP-2 staining (Fig. 2). Tuj-1 was widely recognized as an early neuronal marker, present in the cell bodies, dendrites, and axons of newly differentiated and mature neurons, making it a robust indicator of overall neuronal presence. On the other hand, MAP-2 was predominantly localized in the somatodendritic compartment of mature neurons and is crucial for dendritic plasticity and stability. The concordant increase in both Tuj-1 and MAP-2 positive cells within the ES group not only suggested an enhanced overall survival of transplanted and/or host neurons. It may also potentially indicated a greater degree of neuronal maturation and

dendritic arborization in the presence of ES, which are essential for synaptic integration and functional recovery.

3.3 Acceleration of Axonal Regeneration

GAP-43 immunofluorescence staining was performed to observe regeneration of axons in SCI rats at 8 weeks post-surgery. In the lesion edge, few GAP-43$^+$ axonal fibers were present in the control group, whereas the ES group exhibited a marked increase in GAP-43$^+$ fibers (Fig. 3). However, in the lesion zone, GAP-43$^+$ fibers were almost absent in the control group. In contrast, the percentage of GAP-43$^+$ area in the ES group was significantly increased, although it was only 8.28 ± 2.70 %.

Axonal regeneration post-injury plays a crucial role in SCI repair. During neural development and regeneration, GAP-43 regulates axonal elongation, neurotransmitters release, and strengthening neural plasticity [17]. The immunostaining results showed that ES treatment significantly increased the percentage of GAP-43$^+$ area, both in the lesion core and at the lesion edge, when applied in conjunction with aSCT transplantation. These results indicated that ES could promote axonal regeneration in this therapeutic context. However, within the lesion zone, regenerated axons remain relatively modest (8.28 ± 2.70 %), which may be insufficient to mediate substantial functional recovery (Fig. 1). Therefore, it speculated that the observed functional improvements might also be attributed to other ES-mediated effects, such as enhanced survival of transplanted neurons (Fig. 2), neuroprotection of host neurons, or modulation of the local microenvironment [9-11].

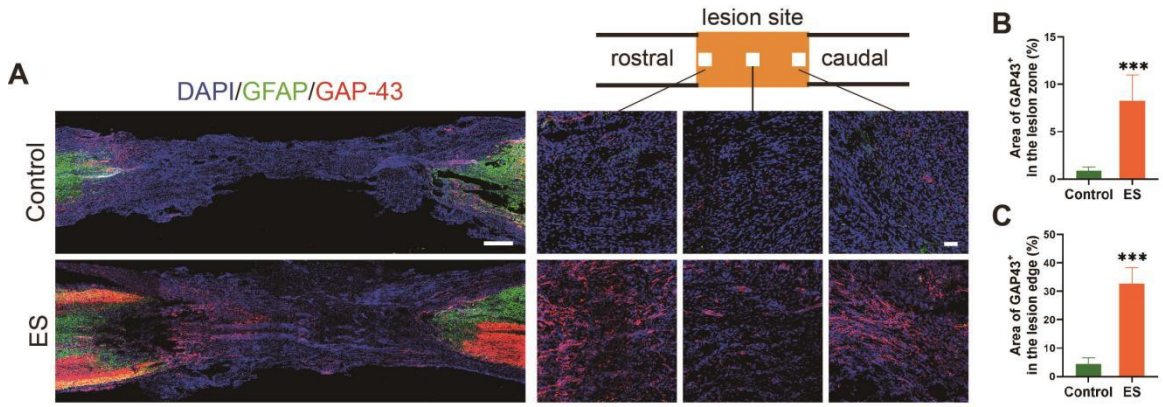

Fig. 3 Assessment of axonal regeneration after SCI. (A) Representative images of GAP-43 immunostaining in different groups at 8 weeks post-surgery. (B) Percentage of GAP-43$^+$ area in the lesion zone. (C) Percentage of GAP-43$^+$ area in the lesion edge. In the left and right images of (A), the scale bars represent 500 μm and 50 μm, respectively. ***$P < 0.001$.

3.4 Investigation of RNA-seq

To further investigate the mechanisms underlying the therapeutic effects, RNA sequencing analysis was performed at 2 weeks post-surgery. A total of 3146 differentially expressed genes (DEGs) were identified in the ES group, among which 2162 genes were upregulated and 984 genes were downregulated ($|\log_2 FC| \geq 1$; p-value ≤0.05, Fig. 4A). DEGs were clustered in a heatmap to highlight transcriptomic differences between control and ES samples (Fig. 4B). GO term analysis showed that DEGs were significantly enriched in extracellular matrix organization, cell adhesion, and axon guidance (biological process category, Fig. 4D), and calcium ion binding (molecular function category, Fig. 4E). KEGG pathway analysis revealed that the DEGs were involved in regulation of neuroactive ligand-receptor interaction, ECM-receptor interaction, calcium signaling, and PI3K-Akt signaling pathways (Fig. 4C). These results suggested that ES may exert its effects by modulating calcium ion homeostasis and apoptosis.

To validate these transcriptomic leads, WB assay was performed to measure the expression levels of key calcium channel and apoptosis-related proteins at 1 and 2 weeks post-surgery. The expression of L-VGCC in the ES group was significantly lower than that in the control group at both time points (Fig. 4F, G). It suggested that ES could attenuate injury-induced calcium influx. In addition, compared to the control group, the expression of cleaved Caspase-3 was also significantly reduced in the ES group at both time points (Fig. 4F, H). It indicated that ES application could inhibit apoptosis, which consistent with our findings of enhanced neuronal survival (Fig. 2).

It is well-established that following SCI, a massive influx of calcium ions occurs, leading to a rapid elevation of intracellular Ca^{2+} concentration. The intracellular calcium overload can trigger a cascade of detrimental events, including the activation of proteases, mitochondrial dysfunction, lipid peroxidation, and the generation of free radicals, which ultimately culminating in neuronal apoptosis and necrosis [7]. It contribute to the formation of an inhibitory microenvironment that hinder neural regeneration. The current results, showing significantly reduced expression of L-VGCC and cleaved Caspase-3 in the ES group, suggested that ES, when combined with aSCT transplantation, could ameliorate the inhibitory microenvironment post-SCI, thereby promoting the recovery of motor function.

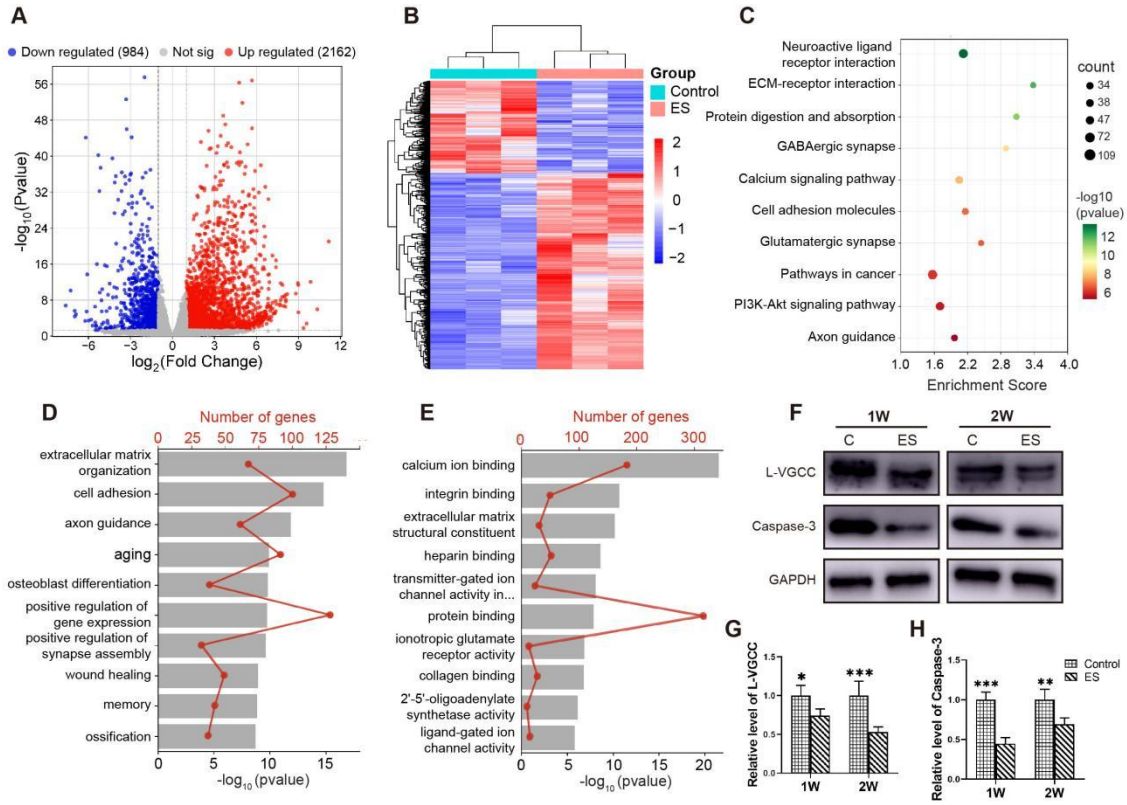

Fig. 4 Investigations of RNA-seq and assessments of protein levels. (A) A volcano plot of RNA-seq results showing DEGs ($|\log_2 FC| \geq 1$; p-value ≤ 0.05). (B) Heatmap of DEGs in ES compared with control group. (C) The gene enrichment KEGG pathway analysis. Top 10 enriched GO biological processes (D), molecular functions (E). Red lines indicate the number of DEGs. (F) WB analysis of L-VGCC and cleaved Caspase-3. (G) Quantitative analysis of L-VGCC. (H) Quantitative analysis of cleaved Caspase-3. $^*P < 0.05$, $^{**}P < 0.01$, $^{***}P < 0.001$.

4. Summary

In this study, the therapeutic potential of ES for complete SCI was investigated, particularly when applied with allogeneic aSCT transplantation. It found that ES significantly enhanced neuronal survival and axonal regeneration in the injured spinal cord, leading to improved locomotor

function recovery. The underlying mechanisms likely involve the ES-mediated modulation of multiple signaling pathways, critically including the attenuation of calcium influx and the inhibition of apoptosis. These actions may contribute to ameliorating the inhibitory post-injury microenvironment. These findings may indicate that ES, when combined with aSCT transplantation, promotes neural repair not only by potentially improving graft viability but also by actively regulating the host responses to injury. This ES-centered therapeutic strategy holds significant promise for facilitating clinical translational research aimed at improving neural function after SCI.

References

[1] Fan B, Wei Z, Yao X, et al. Microenvironment Imbalance of Spinal Cord Injury. Cell Transplant. 2018, 27(6): 853-866.

[2] Anjum A, Yazid MDi, Fauzi Daud M, et al. Spinal Cord Injury: Pathophysiology, Multimolecular Interactions, and Underlying Recovery Mechanisms. Int J Mol Sci. 2020, 21(20): 7533-7568.

[3] Hu X, Xu W, Ren Y, et al. Spinal cord injury: molecular mechanisms and therapeutic interventions. Signal Transduct Target Ther. 2023, 8(1): 245-273.

[4] Shen H, Chen X, Li X, et al. Transplantation of adult spinal cord grafts into spinal cord transected rats improves their locomotor function. Sci China Life Sci. 2019, 62(6): 725-733.

[5] Shen H, Wu S, Chen X, et al. Allotransplantation of adult spinal cord tissues after complete transected spinal cord injury: Long-term survival and functional recovery in canines. Sci China Life Sci. 2020, 63(12):1879-1886.

[6] Gao X, You Z, Li Y, et al. Multifunctional hydrogel modulates the immune microenvironment to improve allogeneic spinal cord tissue survival for complete spinal cord injury repair. Acta Biomater. 2023, 155: 235-246.

[7] Munteanu C, Rotariu M, Turnea M, et al. Main Cations and Cellular Biology of Traumatic Spinal Cord Injury. Cells. 2022, 11(16) :2503-2521.

[8] Xie J, Li J, Ma J, et al. Magnesium Oxide/Poly(l-lactide-co-ε-caprolactone) Scaffolds Loaded with Neural Morphogens Promote Spinal Cord Repair through Targeting the Calcium Influx and Neuronal Differentiation of Neural Stem Cells. Adv Healthc Mater. 2022, 11(15): e2200386.

[9] Zhao P-C, Huang Z-S, Xu S-N, et al. Investigation of the effects of high cervical spinal cord electrical stimulation on improving neurological dysfunction and its potential mechanism in rats with traumatic brain injury. Neuroreport. 2022, 33(12): 509-517.

[10] Dong L, Luan M-Y, Qi Y-N, et al. Calcium homeostasis restoration in pyramidal neurons through micrometer-scale wireless electrical stimulation in spinal cord injured mice. Biochem Biophys Res Commun. 2024, 735: 150487.

[11] Zhu GQ, Jeon SH, Lee KW, et al. Electric Stimulation Hyperthermia Relieves Inflammation via the Suppressor of Cytokine Signaling 3-Toll Like Receptor 4 Pathway in a Prostatitis Rat Model. World J Mens Health. 2020, 38(3): 359-369.

[12] Wang A, Zhang G, Zhang C, et al. Simulation of injury potential compensation by direct current stimulation in rat spinal cord. Biomed Mater Eng. 2014, 24(6): 3693-3700.

[13] Zhang C, Zhang G, Rong W, et al. Early applied electric field stimulation attenuates secondary apoptotic responses and exerts neuroprotective effects in acute spinal cord injury of rats. Neuroscience. 2015, 291: 260-271.

[14] Zhang C, Wang A, Zhang G, et al. Effects of the combination therapy of electric field stimulation and polyethylene glycol in the ex vivo spinal cord of female rats after compression. J Neurosci Res. 2021, 99(7): 1850-1863.

[15] Fan C, Yang W, Zhang L, et al. Restoration of spinal cord biophysical microenvironment for enhancing tissue repair by injury-responsive smart hydrogel. Biomaterials. 2022, 288: 121689-121699.

[16] Liang S, Zhou J, Yu X, et al. Neuronal conversion from glia to replenish the lost neurons. Neural Regen Res. 2024, 19(7): 1446-1453.

[17] Xi K, Gu Y, Tang J, et al. Microenvironment-responsive immunoregulatory electrospun fibers for promoting nerve function recovery. Nat Commun. 2020, 11(1): 4504-4522.